Rear Surface Light Emission Measurements from Laser-produced Shock Waves in Clear and Al-coated Polystyrene Targets

E. A. McLean [d], A. V. Deniz [b], A. J. Schmitt [a], J. A. Stamper [d], S. P. Obenschain [a],
T. Lehecka [b] , A. N. Mostovych [a] , and J. Seely [c]

[a] *Plasma Physics Division, Naval Research Laboratory, Washington, DC 20375, USA*
[b] *Science Applications International Corporation, McLean, VA 22102, USA*
[c] *Space Sciences Division, Naval Research Laboratory, Washington, DC 20375, USA*
[d] *Research Support Instruments, Lanham, MD 20706, USA*

Abstract

The Nike KrF laser, with its very uniform focal distributions, has been used at intensities near 10^{14} W/cm^2 to launch shock waves in polystyrene targets. The rear surface visible light emission differed between clear CH targets and targets with a thin (125 nm) Al coating on the rear side. The uncoated CH targets showed a relatively slowly rising emission followed by a sudden fall when the shock emerges, while the Al-coated targets showed a rapid rise in emission when the shock emerges followed by a slower fall -- allowing an unambiguous determination of the time the shock arrived at the rear surface. A half-aluminized target allowed us to observe this difference in a single shot. The brightness temperature of both the aluminized targets and the non-aluminized targets were slightly below but close to rear surface temperature predictions of a hydrodynamic code. A discussion of preheat effects is given.

Report Documentation Page

1. REPORT DATE **1999**	2. REPORT TYPE	3. DATES COVERED **00-00-1999 to 00-00-1999**

4. TITLE AND SUBTITLE	5a. CONTRACT NUMBER
Rear Surface Light Emission Measurements from Laser-produced Shock Waves in Clear and Al-coated Polystyrene Targets	5b. GRANT NUMBER
	5c. PROGRAM ELEMENT NUMBER
6. AUTHOR(S)	5d. PROJECT NUMBER
	5e. TASK NUMBER
	5f. WORK UNIT NUMBER

7. PERFORMING ORGANIZATION NAME(S) AND ADDRESS(ES) **Naval Research Laboratory,Plasma Physics Division,4555 Overlook Avenue SW,Washington,DC,20375**	8. PERFORMING ORGANIZATION REPORT NUMBER

9. SPONSORING/MONITORING AGENCY NAME(S) AND ADDRESS(ES)	10. SPONSOR/MONITOR'S ACRONYM(S)
	11. SPONSOR/MONITOR'S REPORT NUMBER(S)

12. DISTRIBUTION/AVAILABILITY STATEMENT
Approved for public release; distribution unlimited

13. SUPPLEMENTARY NOTES
Optics Communications, Volume 166, Issues 1-6, 1 August 1999, Pages 141-149

14. ABSTRACT
The Nike KrF laser, with its very uniform focal distributions, has been used at intensities near 1014 W/cm2 to launch shock waves in polystyrene targets. The rear surface visible light emission differed between clear CH targets and targets with a thin (125 nm) Al coating on the rear side. The uncoated CH targets showed a relatively slowly rising emission followed by a sudden fall when the shock emerges, while the Al-coated targets showed a rapid rise in emission when the shock emerges followed by a slower fall -- allowing an unambiguous determination of the time the shock arrived at the rear surface. A half-aluminized target allowed us to observe this difference in a single shot. The brightness temperature of both the aluminized targets and the non-aluminized targets were slightly below but close to rear surface temperature predictions of a hydrodynamic code. A discussion of preheat effects is given.

15. SUBJECT TERMS

16. SECURITY CLASSIFICATION OF:			17. LIMITATION OF ABSTRACT	18. NUMBER OF PAGES	19a. NAME OF RESPONSIBLE PERSON
a. REPORT **unclassified**	b. ABSTRACT **unclassified**	c. THIS PAGE **unclassified**	**Same as Report (SAR)**	**9**	

1. Introduction

Rear surface visible emission can be used to measure shock wave transit times in opaque laser-illuminated targets, because the time of shock breakout can be clearly recorded. It is more of a challenge to obtain accurate interpretations with transparent targets such as polystyrene (CH), which transmit light before the time of shock breakout. Since CH is a common material used in some inertial confinement fusion (ICF) target designs [1], and is used in many ICF experiments, it is important to understand the time evolution of the light emitted, and to have accurate measurements of shock transit times.

This is a paper that describes an optical diagnostic technique to observe shock waves in transparent targets. The shock waves that are produced in CH targets can be investigated by observing the emitted light on the rear side of the target with high speed cameras; however, this light signal is difficult to interpret without accurate time fiducials. To the best of our knowledge, no other group has done an experiment where the same shock wave is observed simultaneously with good time resolution in a target whose rear side is half clear and half coated with a thin layer of aluminum [2]. The aluminum coating is thick enough to stop the visible light. This allows the unambiguous time-resolved observation of the visible light emitted by the shock waves or radiation transport inside the target, and the aluminum coating resolves the question of the time of shock breakout. Accurate shock velocities are needed for equation-of-state studies at ICF multi-megabar pressure conditions.

Because of its very uniform intensity distribution, the Nike KrF laser is particularly well suited for such a study. The measurements of shock transit times are best obtained with flat targets (that simulate a section of a spherical ICF target). The visible emission allows the rear surface temperature to be determined using optical pyrometry, if the plasma is optically thick and near-blackbody conditions are fulfilled [3-9], and these temperatures are compared to those obtained from a radiation hydrocode simulation. Although the measurements and the calculations are presented for one particular shot, similar results were obtained for four other shots with approximately the same conditions. Also, peripheral issues such as preheat are investigated with measurement and theory.

Previous experiments at the Naval Research Laboratory used the Pharos Nd:glass laser (1.06 μm) with thin Al targets [3], but had significant x-ray preheat. Experiments with carbon targets at the Lawrence Livermore National Laboratory on the Shiva laser (predecessor to Nova), also at 1.06 μm wavelength, had significant hot electron preheat [4]. In the present experiment, thick (~58 μm) CH targets with the Nike KrF laser, were expected to be dominated by simple shock heating, with only a small amount of preheat. The short laser wavelength and the smooth laser intensity distribution, both contributed to a reduction in x-ray and electron preheat.

The Nike KrF laser has a UV wavelength of 248 nm, a pulse width of 4 ns, and a focal spot of 750-μm-FWHM diameter, with a flat top ~ 400 μm [2,10]. (The rms fluctuations in the laser flux is ~ 1% rms in each of the overlapped beams. With 37 overlapped beams, the lower mode rms fluctuations are further reduced.)

In this experiment we observed the shock wave breakout light on the rear side of an initially transparent, polystyrene foil target that had one half of the rear side coated with a thin (125-nm-thick) aluminum layer. The Al coating blocked any visible radiation prior to shock breakout. The light emission was observed simultaneously with an optical streak camera and a fast photomultiplier. A laser intensity of $\sim 8 \times 10^{13}$ W/cm^2 produced a calculated shock wave velocity of $\sim 3.3 \times 10^6$ cm/s and a pressure of ~10 Mbar. This shock front was wide enough to overlap the coated and the uncoated regions of the target.

The shock breakout time is verified by a comparison of the emissions from the coated and uncoated sides of the rear surface. For the clear CH targets, we observed a rising level of visible light from the rear surface during the time the shock wave passes through the target, reaching a peak value at shock breakout. After shock breakout, the observed light falls rapidly in intensity. However, the Al-coated CH targets showed only a small light intensity due to x-ray preheat before shock breakout, then a sudden jump in light as the shock breaks out of the target.

The experimental measurements of shock breakout time, back surface temperature, and the effect of preheat, for CH and Al-coated CH targets are compared with computed values using the FAST1D radiation hydrocode simulations for the same experimental conditions. The measured shock breakout times agrees with the simulation values to 10%, and the measured temperatures agree with the simulation to within the experimental error of ± 30%. The x-ray preheat prior to shock breakout in the Al-coated CH target is shown in the simulation.

2. Experiment

The experimental arrangement is shown in Fig. 1. The target chamber is approximately 1 m in radius. The target, positioned in the center of the evacuated chamber, is irradiated with the Nike KrF laser (λ = 248 nm), consisting of 37 overlapping beams. The laser pulse (~1400 J in 37 beams) was focused to a spot 750 microns in diameter FWHM, with a flat central region 400 microns in diameter, producing an intensity of ~ 8 x 10^{13} W/cm^2. The rms spatial variation of a single 4-ns beam has been measured to typically be ~ 1-2% [10]. The 37 overlapping beams should further reduce the spatial variation. The present study had no applied prepulse; however, there is a very low level, <0.1%, ASE or scattered light intensity that precedes the main laser pulse by ~2 ns. (The laser pulse shape is shown in Fig. 2.)

Light emitted from the back side of these targets was relayed with a lens train consisting of two f/10, achromatic, 1.07-m-focal-length lenses that imaged the rear surface without magnification. This image was then relayed with a 38-cm-focal length lens to provide a 3:1 magnification via a beam splitter to both the entrance slit of a streak camera and to a 1-mm aperture in front of a fast (1-ns rise time) photomultiplier. The 1-mm aperture in front of the photomultiplier defined the field of view to ~ 330 μm at the plane of the target, and an interference filter limited the spectral range to 478 nm with a 9-nm bandwidth. The photomultiplier, interference filter, attenuating neutral density filters, and the optical train were calibrated *in situ* to an accuracy of ±15% using a calibrated tungsten strip lamp [3].
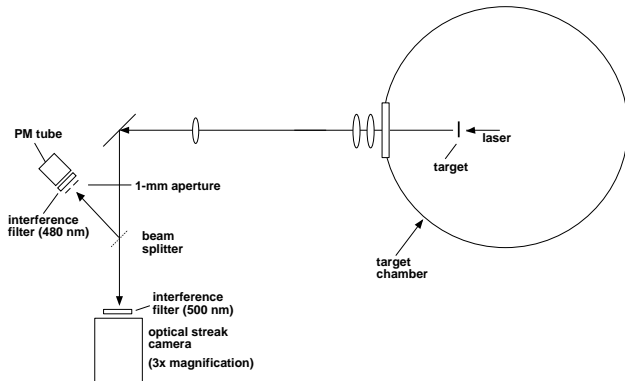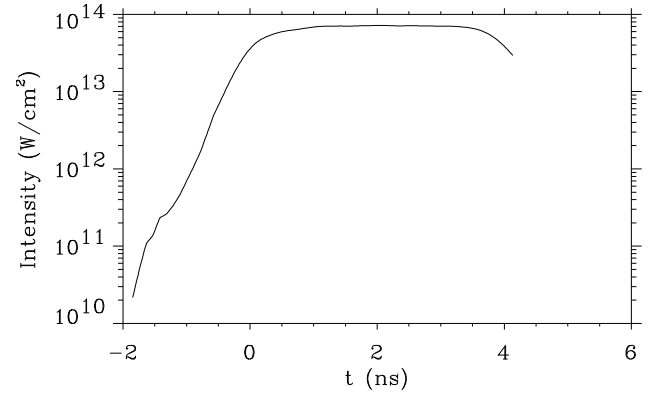

Fig. 1. Experimental arrangement.

Fig.2. Laser pulse shape.

The streak camera was coupled with fiber optics to a cooled CCD camera, and then digitally recorded and analyzed. An entrance slit of 50 microns and a sweep speed of 10 ns/15 mm provided ~80-ps time-resolution with the streak camera. An interference filter limited the spectral range to 500 nm with a bandwidth of 85 nm. There was a secondary intensity calibration of the streak camera made by comparing its signal in a linear range to that of the calibrated photomultiplier, when observing the same light source during a period of slow change. The timing of all the signals was defined so that t = 0 corresponds to the time when the driving laser pulse reaches 50% of peak intensity. The timing accuracy was ± 130 ps.

The target was a transparent CH foil ~ 3 mm wide and 58 μm thick, with an aluminum layer ~1.5 mm wide and 125 nm thick covering one half of the rear side of the target. (The 125 nm of Al blocks visible radiation from passing through the coating.) A 1-D simulation indicates that the 125-nm-Al coating would not materially perturb the shock transit time through the target, but does affect the breakout temperature. Care was taken to assure that the foils were flat and free of blemishes.

3. Experimental Results

For a clear CH target, there is usually an initial small transmission of visible plasma light lasting from about t = -5 ns until t= -0.25 ns. This plasma light is caused by the low intensity laser light (~10^{10} W/cm^2) that precedes the main laser pulse by several nanoseconds. The signal then falls to nearly zero, although the laser light is rising monotonically. This early transmission can be explained as follows: Cold, uncoated CH targets are transparent to optical radiation, but opaque to UV light. (The e-folding depth at a wavelength of 248 nm in CH is ~2 μm, as measured with a spectrophotometer.) The absorption of the early x-

ray and UV radiation produces a plasma in a very thin outer layer of the target that is partially opaque to the optical radiation, so that the transmitted light thus drops to a lower value.

The second portion of the signal begins at t ~ 0 ns. Because of the inferior time resolution (~1 ns) of the photomultiplier compared to that of the streak camera (80 ps), the photomultiplier could not time-resolve the fast rise and fall times of the shock signal. The streak camera was therefore used to obtain a more precise time and intensity comparison of the transparent CH target with the opaque CH-Al targets. A typical streak camera image is shown in Fig. 3a. In the accompanying sketch to the right, the laser beam strikes the top side of the target and the shock wave emerges from the bottom side.
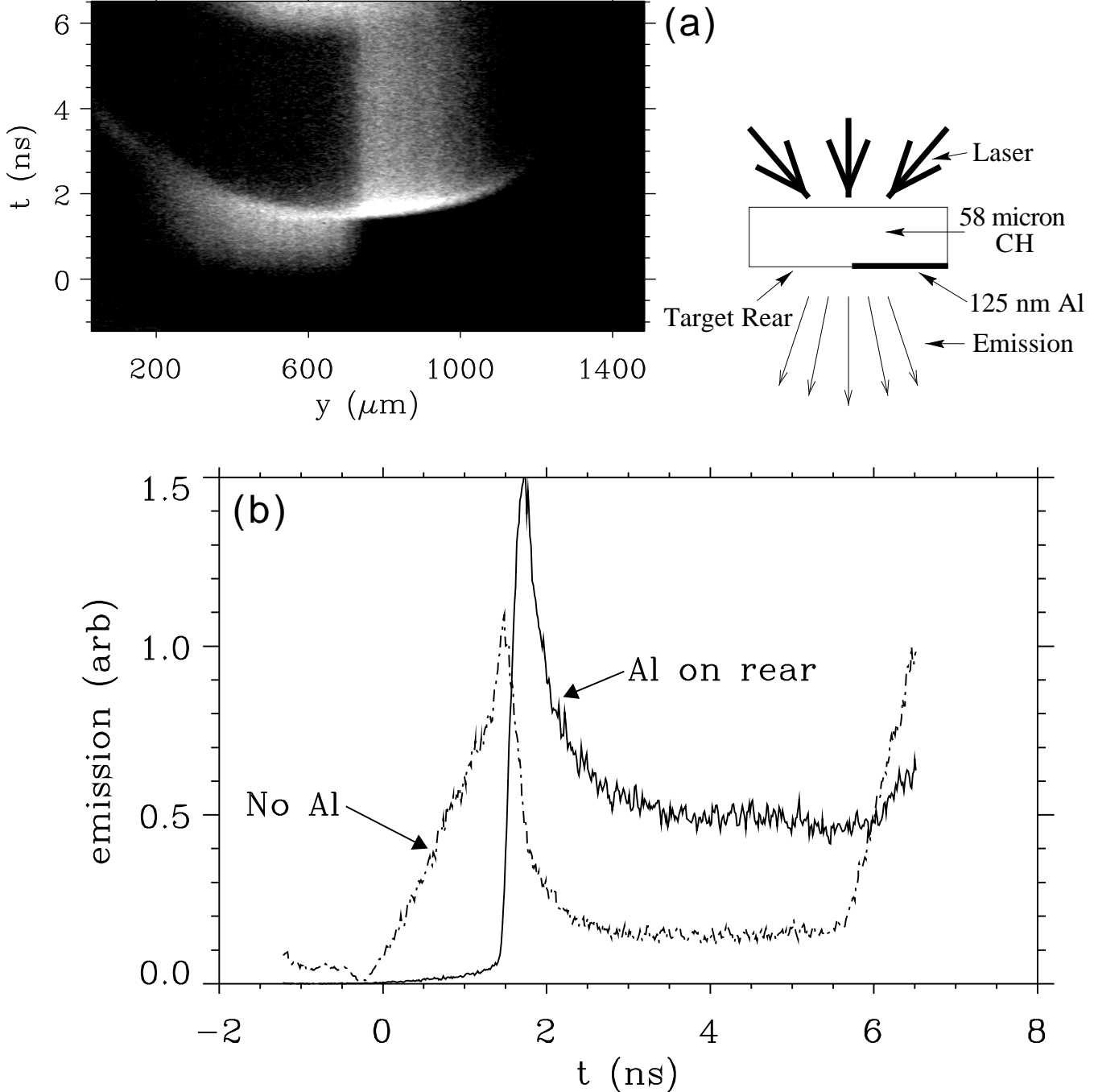

Fig. 3. (a) Streak camera signal of the emission of 500-nm light from the rear of a CH target 58μm thick with a layer of 125-nm-thick Al covering 1/2 of the rear surface as shown in the insert on the right side of the figure. The time t = 0 ns refers to the time of 50% peak intensity of the KrF laser pulse at the plane of the target. The values of y in μm are also at the plane of the target. The left half of streak record shows the clear CH target, and the right half shows the Al coated side of the target. (b) Streak camera lineouts of the above streak record are shown with the solid curve giving the Al-coated lineout, and the dotted curve showing the lineout of the clear side of the target.

Lineouts of the intensity from the Al-coated side of the target and from the uncoated side of the target are shown in Fig. 3b. The target half-coated with Al (solid curve) showed a slowly rising, low intensity emission between t = 0 and t =1.45 ns. We believe this is due to preheat from the x-ray radiation emanating from the front side plasma. Calculations indicate that the aluminum layer could absorb enough x-ray radiation in the 2 - 3 keV region to heat the Al to well above its melting temperature. At lower photon energies, the CH foil absorbs most of the x-ray flux before it reaches the aluminum coating. At higher photon energies, the absorbed x-ray flux is insufficient to melt the aluminum coating. The temperature inferred from the streak camera data of the light intensity emitted from this preheated region at t ~ 1.25 ns is 0.8 eV.

When the shock wave first breaks out of the Al-coated rear side at t ~ 1.4 ns the light intensity rises very rapidly to a peak at t = 1.7 ns. The light then begins to be absorbed by the rarefaction wave[11] and decays to about 1/3 of its peak value. We assume the shock breakout time occurs at t = 1.45 ns, which is at 10% of the peak intensity of the Al-coated side and approximately at the peak of the pure CH signal. . The rise time of the shock breakout light is ~ 180 ps, which is about 2 times longer than the streak camera time resolution (80 ps). This is the rise time measured between the 10% and 90% intensity level of the peak. This rise time is slower than expected from simple theory (~1 ps). The reason for this slow rise time is probably associated with the preheat and its expansion of the rear surface.

The uncoated portion of the target behaved quite differently. Light can be observed on the streak camera image from before t ~ 0 ns, dipping to zero at t = -0.25 ns, and then increasing to a peak at 1.45 ns. Then the light intensity decays rapidly to a lower level (<15% of peak intensity). We believe that the shock breakout time for the uncoated side of the target occurred near the time of the peak light intensity. In an experiment using indirect drive from a laser-driven hohlraum to produce a shock wave in transparent Parylene-C, Evans et al. [12] also noted that the shock breakout from the Parylene-C was indicated by a similar fall in luminosity.

If the 480-nm-light emitted in the CH from t = 0 ns to t = 1.4 ns is assumed to come only from the shock wave, it should be of approximately constant intensity as it passes through the target. Since this light as observed from the rear of the target is steadily increasing as it approaches the rear surface, it is possible to estimate the absorption length of the shock light during its passage through the preheated target, assuming that the CH ahead of the shock is uniformly absorptive. This was done and the absorption length was found to be 21 microns. (This is shorter than the absorption length measured with room temperature CH, which is 970 μm.) Now we turn our attention to a description of the hydrocode simulation for the same conditions used for the experiment.

4. Description of the FAST1D hydrocode

The FAST1D radiation hydrocode was used to simulate the CH and Al-coated CH targets under these experimental conditions. The FAST1D code solves the 1-dimensional fluid equations (conservation of mass, momentum, and energy) for the material, and includes: electron and ion conductivity and electron-ion equilibration; real-material Equation of State (EOS) data from table look-ups, radiation transport; and calculates shock heating with a tensor artificial viscosity description [13]. The flux corrected-transport (FCT) [14] algorithms are used to solve for the advection of the fluid variables. This algorithm is implemented on an Eulerian mesh that is allowed to move in an arbitrary manner, allowing one to keep areas such as the back end of the target highly resolved throughout the simulation.

Thermal conductivities are modeled by a flux-limited Spitzer-Härm description, with flux-limiters of 10% and 65% of free-streaming applied to electrons and ions, respectively. (The ion heat-flux is negligible for all of the simulations reported here.) The EOS is based on the CHARTD EOS model [15], and uses Thomas-Fermi and Saha average-atom ionization electron modeling and a Debye-Grüneisen atom/ion model, with modifications to account for pressure ionization. Laser deposition in the underdense coronal region is calculated assuming inverse bremsstrahlung absorption and uses raytracing to correctly account for non-normally incident light. Finally, (non-laser) radiation transport is handled by a multigroup diffusion algorithm using a variable Eddington factor [16]. The opacities used in this multigroup method are assumed to be Local Thermal Equilibrium (LTE) and are calculated using the NRL-STA code [17].

5. Comparison of numerical results with the experiment

A qualitative picture of the shock process is given by a mass flow plot obtained from the hydrocode simulation as shown in Fig. 4. Here the mass density is plotted as a function of time and distance perpendicular to the target; the gray scale denotes the target mass density, with the lighter shades referring to the lower densities. At t ~ -2 ns on this plot a weak shock is formed during the rise of the pulse, that compresses the front side of the target about 20% before being overtaken by the strong shock from the high intensity portion of the laser pulse. This strong shock has a velocity of ~3.3 x 10^6 cm/sec and breaks out of the rear surface of the target at t ~ 1.33 ns.

From the simulation, the density, temperature, and pressure as a function of distance are shown in Fig. 5 for four times ranging from t = -1.85 ns, the time just before the laser strikes the target, to t = +1.37 ns, just after the shock breaks out of the rear surface of the target. The solid line represents t = -1.85 ns, and the dot-dash line

Fig. 5. Computed curves are shown for the density, the electron temperature, and the pressure versus distance for various times. The rear surface of the target is initially at z = 100 μm. The times on these plots are -1.85 ns (solid curve), -0.3 ns (dotted curves), +0.55 ns (dashed curves), and +1.37 ns (dot - dash curves). The main laser pulse reaches 50% maximum intensity at t = 0 ns. Shock breakout occurs just before t = 1.37 ns.
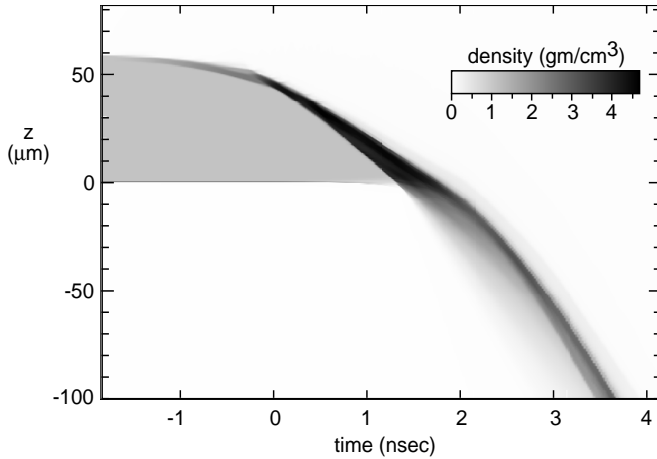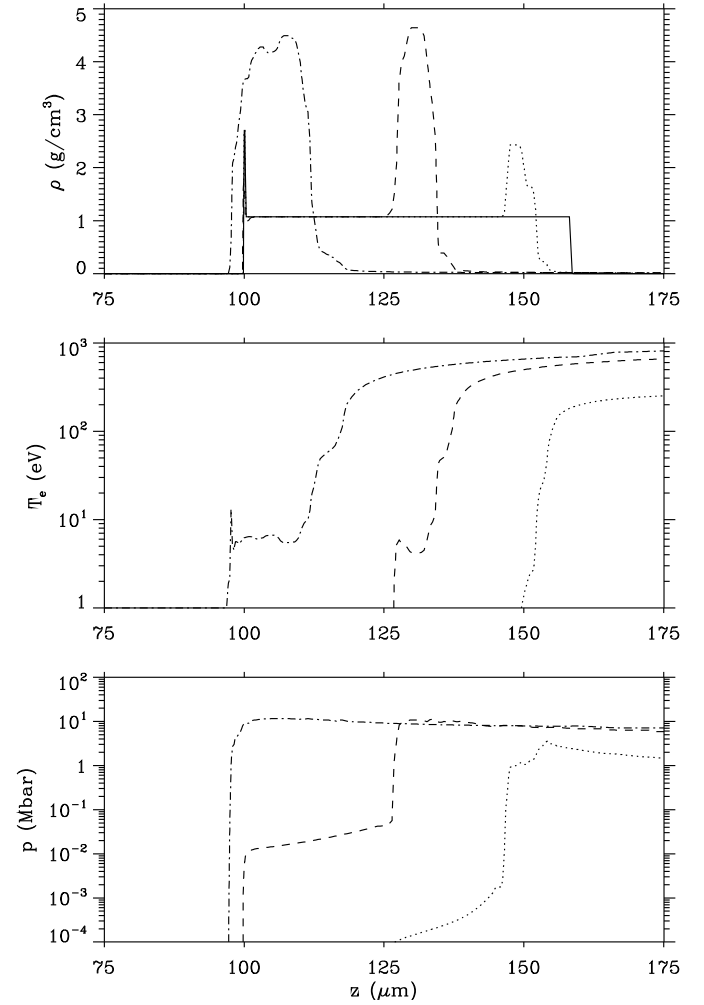

Fig. 4. Hydrocode 1-D simulations of shock waves in a polystyrene foil showing the mass density as a function of time and distance perpendicular to the target. Darker shades on the plot represent higher target densities. The driving laser comes from the top of the target. The rear surface of the target is initially at z = 0 μm. The target is a 58-μm-thick CH foil with a 125-nm-thick Al coating on the rear side of the target. The diameter of the laser focal spot is 750 μm and the intensity is 8 x 10^{13} W/cm^2. The main laser pulse begins at about t = -0.25 ns and shock breakout occurs at about t = +1.33 ns.

represents t = +1.37 ns. The laser beam comes from the right side. In the plot ρ vs. z, the solid line (t = -1.85 ns) shows the density of the 58-μm-thick CH including the 0.125-μm-thick aluminum layer on the rear side of the target. At t = -0.3 ns (the dotted curve) shows the starting compression of the target due to the low laser intensity (~ 1.3 x 10^{13} W/cm^2) at that time. At t = -0.3 ns, the temperature of the plasma plume at the front of the target has risen to ~250 eV. The effects of the main laser pulse are beginning at t = +0.55 ns (the dashed curve), when a more energetic shock wave is starting to pass

through the target, and the corona temperature at the front of the target has reached ~600 eV. The target thickness at that time has decreased from a starting thickness of 58 μm to a thickness of 38 μm and there is a region of higher density.

From these discrete time frames, the shock breaks out of the rear of the target around t = 1.37 ns. The pressure rises to 10 Mbar and the temperature of the shock breakout has a very short time-duration peak of 10 eV. The compressed target material is now starting to show acceleration away from the laser.
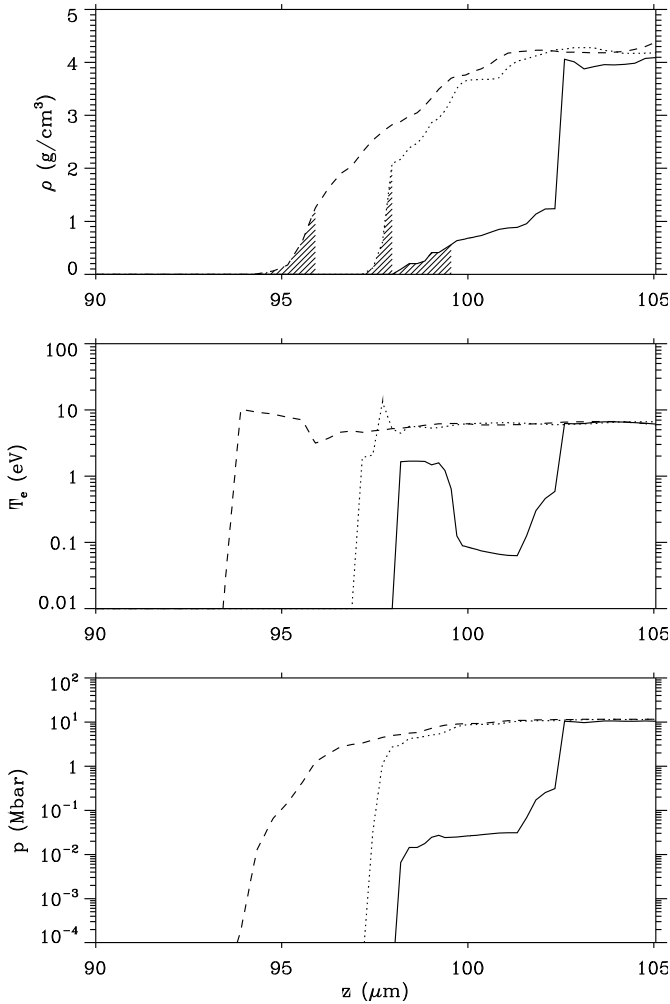
Fig. 6. Similar computed curves to those in Fig. 5, but with a large expansion of the distance and much finer time steps to highlight the effect of the preheat of the aluminum layer. The rear surface of the target is initially at z = 100 μm. The aluminum is shown as the shaded regions. The times on these plots are +1.25 ns (solid curves), +1.37 ns (dotted curves), and +1.42 ns (dashed curves). The effect of preheat can be seen in the initial expansion of the aluminum layer and the temperature rise prior to the shock reaching the rear surface.

Since changes, particularly in the Al layer, are occurring so rapidly, three times in the interval +1.25 ns to +1.42 ns are shown in Fig. 6. Also, the distance scale (z) has been expanded. The Al layer is shown as the shaded region. One can now see the effects of the preheat on the aluminum coating on the rear side of the target. At t = 1.25 ns (the solid curve), before the shock reaches the aluminum layer, the aluminum has started to get heated by the x-ray radiation from the front plasma plume. The peak density of the Al has dropped to about 0.5 g/cm^3 and the width of the layer has expanded ~ 12 times to ~ 1.5 μm. The temperature of the Al coating is ~1.5 eV. (The decrease in the Al density and the increase in the temperature due to the preheat, increases the optical depth, and thus could increase the emission rise time during shock breakout.) As time proceeds, the shock wave compresses the aluminum layer and the density rises until it reaches 2 g/cm^3 at 1.37 ns (the dotted curve), which is near the time of shock breakout. Also at this time there is a spike in the temperature, rising briefly to over 10 eV. At t = 1.42 ns (the dashed curve), the Al layer is again decompressing.

Figures 5 and 6 show the calculated effect of the radiation preheat on the heating and compression processes at this laser intensity level (8 x 10^{13} W/cm^2). The heating of the aluminum layer in the simulation (~1.5 eV) agrees roughly with the temperature inferred from the rear surface emission measurements (~0.8 eV).

To get a more accurate determination of the peak temperature of the Al-coated targets, three targets with a full aluminum coating on the rear side of the target were hit by the laser beam with similar conditions. The average peak temperature determined from the streak camera data of the visible light emission was 7 eV ±30%. The numerical simulation predicted 10 eV for a very short time. (It may be that we do not have adequate time resolution to follow precisely the intensity changes, or that the blowoff material is absorbing some of the emitted light.) However, to the accuracy of measurement (±30), the temperature measurement of the Al-coated CH target agreed with the simulation. Also, similar measurements were made for the pure CH targets and the average temperature was found to be 4.3 eV. The simulation gave a peak temperature of 5.5 eV, which is about the same ratio higher as that found for the Al-coated targets.

7. Conclusions

Using the very smooth laser pulse from the Nike KrF laser, we have observed a laser-produced shock wave in a special CH foil target that has half of the rear side covered with a thin layer of aluminum. With the clear half of the target, the observed light includes the initial light from the front of the target, the light from the shock wave as it passes through the target, and the light as the shock wave breaks out of the rear side of the target. The Al coating gives a well-defined time of shock breakout, and this is compared with the light signal from the transparent target. This result verifies that for CH, the shock breakout time is characterized by a sudden reduction in light emission. The 1-D radiation hydrocode calculation using the same conditions as those in the experiment yields a shock breakout time which is within 10% of the experimental measurement.

Absolute light intensity measurements from both the coated and the uncoated targets allowed rear side temperatures to be determined, which are also compared to the hydrodynamic calculations. The rear side temperatures for both the Al-coated and the uncoated targets are 20 - 30% lower than the temperatures determined by our radiation hydrodynamics code; however, to the accuracy of the measurements ($\pm30\%$), the measured and the calculated temperatures are in agreement. Prior to shock breakout the Al-coated target produces a small rear side emission due to x-ray preheat (preheat is also seen in the simulation). The measured and calculated preheat temperatures (~ 1 eV) are in rough agreement.

8. References

[1] R.J. Mason, R.A. Kopp, H.X. Vu, R.G. Watt, D.Wilson, and O. Willi, Bull. APS **41** (1996) 1526.

[2] A.V. Deniz, T. Lehecka, E.A. McLean, S.P. Obenschain, J.A. Stamper, A.J. Schmitt, J.D. Sethian, K.A. Gerber, C.J. Pawley, V. Serlin, R.H.Lehmberg, S.E. Bodner, C.A. Sullivan, A.N. Mostovych, J.P. Dahlburg, and J.H. Gardner, Bull. APS **41** (1996).

[3] E.A. McLean, S.H. Gold, J.A. Stamper, R.R. Whitlock, H.R. Griem, S.P. Obenschain, B.H. Ripin, S.E. Bodner, M.J. Herbst, S.J. Gitomer, and M.K. Matzen, Phys. Rev. Lett. **45** (1980) 1246.

[4] S.P. Obenschain, R.R. Whitlock, E.A. McLean, B.H. Ripin, R.H. Price, D.W, Philion, E.M. Campbell, M.D. Rosen, and J.M.Auerbach, Phys. Rev. Lett. 50 (1983) 44; S.H. Gold and E.A. McLean, J. Appl. Phys. **53** (1982) 784.

[5] A. Ng, D. Parfeniuk, L. DaSilva, and D. Pasini, Phys. Fluids 28 (1985) 2915; L. DaSilva, A. Ng, and D. Parfenik, J. Appl. Phys. **58** (1985) 3634.

[6] David Salzmann, Henry Szichman, Aaron D. Krumbein, and Clarence E. Capjack, Phys. Fluids **30** (1987) 515.

[7] H. Pepin, R. Fabbro, B. Faral, J. Virmont, F. Cottet, and J.P. Romain, Phys. Fluids **28** (1985) 3393.

[8] M. H. Key, Handbook of Plasma Physics, Eds. M. N. Rosenbluth and R. Z. Sagdeev, Vol. **3**: Physics of Laser Plasma, edited by A. M. Rubenchik and S. Witkowski (Elsevier Science Publishers B. V. ,1991)

[9] Ya. B. Zel'dovich, S.B. Kormer, M.V. Sinitsyn, and A.I. Kuriapin, Sov. Phys. Doklady **3** (1958) 938.

[10] S.P. Obenschain, S.E. Bodner, D. Colombant, K. Gerber, R.H. Lehmberg, E.A. McLean, A.N. Mostovych, M.S. Pronko, C.J. Pawley, A.J. Schmitt, J.D. Sethian, V. Serlin, J.A. Stamper, C.A. Sullivan, J.P. Dahlburg, J.H. Gardner, Y. Chan, A.V. Deniz, J. Hardgrove, T. Lehecka, and M. Klapisch, Phys. Plasmas **3** (1996) 2098.

[11] Ya.B. Zel'dovich and Yu.P. Raizer, Physics of shock waves and high-temperature hydrodynamic phenomena (Academic Press, New York, 1966).

[12] A.M. Evans, N.J. Freeman, P. Graham, C.J. Horsfield, S.D. Rothman, B.R. Thomas, and A.J. Tyrrell, Laser and Particle Beams **14** (1996) 113.

[13] W. F. Noh, J. Comp. Phys. **72** (1987) 78; P. P. Whalen, LANL memo X-DO-PPW(3/84)-02, March 1984.

[14] D. L. Book, J. P. Boris, and K. J. Hain, J. Comp. Phys. **18** (1975) 248.

[15] S. L. Thompson, and H. S. Lauson, *"Improvement in CHART D Radiation-hydrodynamic code III: revised analytic equations of state"* SC-RR-71 0714, Sandia Laboratories, Albuquerque, New Mexico, March 1972.

[16] J. P. Dahlburg, M. Klapisch, J. H. Gardner, C. R. DeVore, A. J. Schmitt, and A. J. Bar-Shalom, J. Quant. Spectrosc. Radiat. Transfer **54** (1995) 113.

[17] A. Bar-Shalom, J. Oreg, W. H. Goldstein, D. Shvarts, A. Zigler, Phys. Rev. **A 40** (1989) 3183.